Journal of Mining and Environment (JME) Vol. 17, No. 5, 2026, 1825-1842

Shahrood University of Technology

Journal of Mining and Environment (JME)

Journal homepage: www.jme.shahroodut.ac.ir

Iranian Society of Mining Engineering (IRSME)

Enhanced Flyrock Prediction in Blasting Operations via Artificial Neural Networks and Hybrid Metaheuristic Optimization

Jalil Hanifehnia[1], Akbar Esmaeilzadeh[2*], Solat Atalou[3], and Reza Mikaeil[4]

1. Department of Mining Engineering, Ah.C., Islamic Azad University, Ahar, Iran
2. Department of Mining Engineering, Faculty of Environment, Urmia University of Technology, Urmia, Iran
3. Department of Mining Engineering, Ah.C., Islamic Azad University, Ahar, Iran
4. Department of Mining Engineering, Faculty of Environment, Urmia University of Technology, Urmia, Iran

Article Info

Received 9 August 2025

Received in Revised form 31 August 2025

Accepted 29 December 2025

Published online 29 December 2025

DOI: 10.22044/jme.2025.16642.3261

Keywords

Flyrock

Environmental issue

Imperialist competitive algorithm

Ant colony optimization

Sungun copper mine

Abstract

Blasting is a crucial technique in mining for rock fragmentation, but it can lead to environmental impacts like vibrations, flyrock, and backbreak. Accurately predicting and controlling these effects is essential for improving safety and minimizing damage to equipment and infrastructure. This research aims to predict flyrock distances (FR) at the Sungun Copper Mine through the application of artificial intelligence (AI) models in conjunction with statistical approaches. Initially, a linear multivariate regression (LMR) model was constructed to establish the correlation between blasting parameters and flyrock range. Subsequently, an artificial neural network based on a multilayer perceptron (ANN-MLP) was developed and further optimized using two advanced hybrid algorithms: the Imperialist Competitive Algorithm (ICA) and Ant Colony Optimization (ACO). These algorithms were employed to calibrate the neural network's weights and biases using variables such as number of blast holes, hole spacing, burden, total charge, specific drilling, charge per hole, and specific charge. Results showed that the ANN-MLP model outperformed the LMR model, with performance metrics of root mean square error (RMSE = 9.31 m), mean absolute error (MAE = 7.10 m), and coefficient of determination (R^2 = 0.81) during the test phase. However, optimization of the ANN model with ICA and ACO significantly improved prediction accuracy. Among the hybrid models, the ICA-ANN model performed best with RMSE = 5.66 m, MAE = 4.60 m, and R^2 = 0.89, showing a considerable improvement over the LMR and ANN-MLP models. Sensitivity analysis further highlighted total charge and number of holes as the most influential parameters affecting flyrock dispersion. Overall, the findings underscore the potential of hybrid AI frameworks in advancing predictive modeling for safer and more efficient blasting operations.

1. Introduction

Drilling and blasting remain the most widely adopted techniques in both mining and construction sectors, primarily due to their cost-efficiency, operational flexibility, and adaptability across a broad spectrum of geological conditions [1]. When properly executed, blasting operations not only achieve efficient rock fragmentation but also play a vital role in minimizing environmental disturbances particularly ground vibrations and flyrock distance which can lead to severe unintended consequences if not adequately controlled [2]. Therefore, a comprehensive understanding of the factors and parameters influencing these events is essential for optimizing blast outcomes. Flyrock distance (FR), a frequently encountered and unpredictable result of blasting in open-pit mines, refers to the uncontrolled projection of rock fragments following detonation. This phenomenon can cause significant damage to surrounding structures, equipment, and even endanger personnel, making it a major safety concern in mining operations [3]. A wide range of

Corresponding author: aesmail.1985@gmail.com (A. Esmaeilzadeh)

empirical models have been developed over the decades to estimate flyrock distance behavior by incorporating various blasting parameters [4-8]. However, many of these models are constrained by their reliance on a limited number of input variables, which often compromises their predictive accuracy and overall robustness. This limitation underscores the necessity for more sophisticated and integrative modeling approaches to enhance the reliability of flyrock distance prediction. To address this challenge, researchers have explored a variety of computational and mathematical methodologies, including artificial neural networks (ANN), fuzzy inference systems (FIS), Monte Carlo simulation techniques, multiple linear regression, support vector machines (SVM), rock engineering systems (RES), and adaptive neuro-fuzzy inference systems (ANFIS) [9-12]. Despite their individual strengths, these models highlight ongoing gaps in achieving high-precision flyrock distance forecasting, particularly under complex geological and operational conditions. Recent advancements in artificial intelligence (AI) and soft computing (SC) techniques have opened new avenues for more accurate and data-driven prediction of flyrock distance in blasting operations [13-17]. For example, Jiang et al. [18] constructed an ANN model integrating parameters such as blast design, rock mechanics, and geological features, achieving high predictive performance and reinforcing the model's potential for mitigating flyrock-related risks. Similarly, Koopialipoor et al. [19] utilized hybrid intelligence frameworks combining genetic algorithms (GA), particle swarm optimization (PSO), and the Imperialist Competitive Algorithm (ICA) to refine blast design variables. Their study concluded that the ANN-PSO model delivered superior accuracy, identifying hole diameter as the most critical parameter influencing flyrock distance. Furthermore, Nguyen et al. [20] introduced an ensemble artificial neural network (EANN) model validated over 210 datasets, which demonstrated higher accuracy than conventional ANN architectures. Rad et al. [21] applied least squares support vector machines (LS-SVM) to predict flyrock distance in blasting operations at the Gol-E-Gohar iron mine, outperforming conventional support vector regression (SVR). Sensitivity analysis indicated powder factor and rock density as the most influential parameters. Rezaei et al. [22] developed a PCA-CART model to predict flyrock distance in open-pit blasting at the Sangan iron mine, achieving high accuracy (R^2 = 0.94). Sensitivity analysis identified specific charge and spacing as the most and least influential parameters, respectively, and the study proposed optimized blasting guidelines that significantly reduced flyrock distance occurrences. Nikafshan Rad et al. [23] proposed an optimized blasting design aimed at minimizing flyrock distance by integrating Recurrent Fuzzy Neural Networks (RFNN) with Genetic Algorithms (GA) in the Shour River Dam mine. Their hybrid model, trained on 70 datasets, demonstrated superior predictive capabilities compared to nonlinear regression techniques. Sensitivity analysis highlighted the critical influence of specific charge on flyrock distance outcomes. Rezaei et al. [24] developed a Mamdani fuzzy model to predict flyrock distance in surface mining operations at the Gol-E-Gohar iron mine, demonstrating superior performance over conventional statistical methods. Sensitivity analysis identified powder factor as the most influential parameter and rock density as the least. In another study, Zangoei et al. [25] applied ICA to optimize a three-layer ANN for predicting flyrock distances, achieving high correlation coefficients and prediction reliability. Zhou et al. [26] explored a range of hybrid machine learning models by combining Support Vector Regression (SVR) with several metaheuristic algorithms, such as the Gravitational Search Algorithm (GSA), Whale Optimization Algorithm (WOA), and Biogeography-Based Optimization (BBO). Their experimental analysis, conducted on datasets from Iranian surface mines, revealed that the SVR-WOA hybrid model provided the highest predictive accuracy, with the lowest Root Mean Square Error (RMSE). Likewise, Zhang et al. [27] introduced a stacked Multiple Kernel Support Vector Machine (MK-SVM) model, which achieved excellent predictive outcomes with low RMSE and MAE values, along with high Variance Accounted For (VAF) during both training and testing phases.

The growing body of literature confirms the effectiveness of Artificial Intelligence (AI) and Machine Learning (ML) in modeling complex flyrock behavior in blasting operations. A key trend in recent studies is the development of hybrid models that integrate metaheuristic optimization techniques with machine learning architectures to overcome limitations of conventional models. While Artificial Neural Networks (ANN) are powerful in nonlinear pattern recognition, they often suffer from slow convergence and the risk of entrapment in local optima. To counter these drawbacks, metaheuristic algorithms iteratively update ANN parameters through flexible, stochastic processes, enhancing generalization and

predictive accuracy. Notable research in this domain includes works by Kalaivaani et al. [28], Murlidhar et al. [29], and Hasanipanah et al. [30], who employed metaheuristic approaches such as Particle Swarm Optimization (PSO), Harris Hawks Optimization (HHO), and the Adaptive Dynamical Harmony Search (HS) algorithm to develop robust hybrid ANN models. These techniques have proven effective in overcoming the traditional shortcomings of ANN and yielded enhanced model performance in highly uncertain and dynamic blasting environments. Given the inherent variability and uncertainty in mine blasting operations, achieving fully deterministic predictions of flyrock distance is exceptionally challenging. The complex interactions among geological, design, and operational factors limit the applicability of purely deterministic models. As such, the incorporation of AI-based hybrid approaches offers a promising direction for improving prediction reliability. By optimizing blast parameters, such models can substantially improve both the safety and efficiency of blasting activities. In the present study, a two-stage modeling approach was adopted to predict flyrock distances at the Sungun Copper Mine in Iran. Initially, a Linear Multivariate Regression (LMR) model was developed to establish baseline predictive performance. Subsequently, two hybrid models ICA-ANN and ACO-ANN were constructed. The Imperialist Competitive Algorithm (ICA), inspired by sociopolitical evolution, and the Ant Colony Optimization (ACO), modeled on the foraging behavior of ants, were employed to optimize the ANN's weights and biases. These algorithms have been successfully applied in various engineering optimization problems. Their integration into the ANN framework in this study was aimed at addressing the known limitations of traditional neural networks and producing a robust predictive model for flyrock distance estimation.

2. Materials and Methods

2.1. Case Study

The Sungun Copper Mine is situated in East Azerbaijan Province, Iran, approximately 73 kilometers northwest of Ahar city, at geographic coordinates 46°43′E longitude and 38°42′N latitude (see Figure 1). Positioned at an elevation of 2,390 meters above sea level, the mine lies within the geologically significant Alpine–Himalayan copper belt, a region renowned for its extensive mineralization and abundant copper reserves. The mine primarily extracts copper and molybdenum, with by-products such as gold and silver. It holds substantial reserves, estimated at 796 million tonnes of ore, with 388 million tonnes classified as proved reserves, at a copper grade of 0.67%. These figures underscore the mine's importance as a significant source of copper in the region. The mining operation employs an open-pit extraction method, which is commonly used for large-scale copper mining operations. The working benches are designed with a height of 12.5 meters and a slope of 68°, while the overall slope of the open-pit mine is 37°, providing a stable and efficient excavation environment. The ramps, which ensure accessibility and haulage efficiency, have a width of 30 meters and a slope of 5°. Currently, the mine has been in operation for approximately 32 years.

Figure 1. Geographical location of the Sungun copper mine with blasting operations and rock fragments

At Sungun Copper Mine, rock fragmentation is primarily achieved through bench blasting using ANFO explosives placed in blast holes along free faces. The blasting process initially utilized detonating cords to ensure simultaneous ignition of the caps. A triangular drilling pattern was mainly adopted, with the burden-to-spacing ratio tailored to the unique conditions of each blast block within different areas of the mine. One of the major challenges during blasting here is the occurrence of flyrock distance, which poses safety and operational concerns. Therefore, this research aims to create a predictive model for estimating flyrock travel distance by applying metaheuristic optimization techniques.

2.2. Dataset Description

Advanced analytical methods, such as correlation analysis, multiple regression, and analysis of variance (ANOVA), which are parametric tests, typically assume that the data

follow a normal distribution. According to Ghasemi and Zahediasl [31], when the sample size exceeds 30 or 40, deviations from the normality assumption generally do not significantly impact the results. Additionally, to visually assess the distribution of data and check for normality, researchers often employ box plots, which also help in identifying outliers. This study determined both input and output parameters after the data collection process. The dataset includes records from 308 blasting operations conducted at the Sungun Copper Mine between April and December 2018, along with their associated flyrock distances. Figure 2 displays box plots summarizing the dataset. Several input parameters, including specific drilling (SD), total charge (TC), specific charge (SC), and charge per hole (CPH), show the presence of outliers, which are observable in the plots. Therefore, it is necessary to remove these outlier values from the dataset to prevent potential bias or deviation in the modeling process.

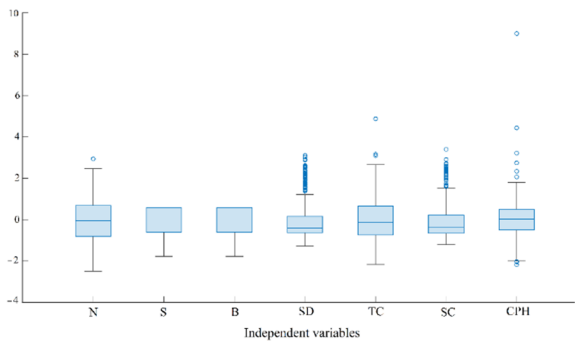

Figure 2. Box plot of input parameters.

The Z-score method was applied to detect and remove outliers from the dataset. This statistical technique calculates how far a data value deviates from the mean in terms of standard deviations. By using this approach, it becomes possible to determine whether a value lies within the normal distribution range or if it is significantly different, thus identifying it as an outlier. The Z-score is calculated using the following equation [32], and values exceeding a threshold of typically ±3 standard deviations are considered indicative of outliers that may distort the integrity of the analysis. By removing these outlier points, the analysis becomes more robust and reliable.

$$Z = \frac{x - \mu}{\sigma} \tag{1}$$

where μ represents the mean of the dataset, and σ indicates the standard deviation. Data points that deviated by more than three standard deviations from the mean were identified as outliers and subsequently excluded from the analysis. The threshold of three standard deviations was chosen, as it is a common criterion in statistical analysis for detecting extreme values that may distort the model's performance. After removing these outliers, 205 data points remained for further investigation. Each blast was characterized by several parameters. The rock mass is predominantly copper-bearing ore with relatively uniform density, lithology, and jointing; uniaxial compressive strength (UCS) is assumed consistent across the studied benches [17, 33]. All blasts used ANFO explosives with detonating cords for simultaneous initiation, and explosive parameters such as charge per hole (CPH), total charge (TC), and specific charge (SC) were recorded. Stemming lengths were relatively uniform within each blast block and therefore not included as independent variables. Blasting geometry parameters, including burden (B), spacing (S), number of holes (N), and hole depth, were recorded. Hole diameter was constant (6.5 inches) across all blasts. Operational parameters, such as specific drilling (SD) and inter-row delay (42 ms), were documented; inter-hole delay was zero, and inter-row delay showed no variability [17], so these were excluded from modeling. Statistical properties of the cleaned dataset, including mean, standard deviation, minimum, and maximum for each parameter, are summarized in Table 1

Table 1. Effects of variables on estimating flyrock distance using 205 observations after outlier removal.

Parameters	Type of parameter	Unit	Symbol	Maximum	Minimum	Mean	Standard deviation
Number of holes	Input	Loop	N	61	3	29.84	10.84
Spacing	Input	m	S	6	4	5.52	0.84
Burden	Input	m	B	3	3	4.52	0.84
Specific drilling	Input	m/m^3	SD	0.08	0.02	0.04	0.01
Total charge	Input	kg	TC	7000	270	3225	1375
Specific charge	Input	kg/m^3	SC	875.45	203.19	38.54	15.75
Charge per hole	Input	kg	CPH	23.34	10.71	14.69	1.60
Flyrock distance	Output	m	FR	140	40	18.28	18.28

The dataset was divided into training and testing subsets for model development and evaluation. Specifically, 80% of the data (163 records) was randomly selected to train the predictive model, while the remaining 20% (42 records) was reserved as a testing set to assess model performance and generalization capability. No separate validation set was used, as model tuning was performed within the training set using cross-validation. Model performance in forecasting flyrock distance was assessed using three key indicators: Root Mean Square Error (RMSE), Mean Absolute Error (MAE), and the coefficient of determination (R^2). An effective predictive model is characterized by a low RMSE, indicating minimal deviations between predictions and actual values, alongside an R^2 value approaching unity, which reflects a high degree of correlation between observed and predicted outcomes. The mathematical expressions for these evaluation metrics are presented below [34-35]:

$$RMSE = \sqrt{\frac{1}{N}\sum_{i=1}^{N}(X_{i,pred} - X_{i,meas})^2} \quad (2)$$

$$MAE = \frac{1}{N}\sum_{i=1}^{N}\left|X_{i,meas} - X_{i,pred}\right| \quad (3)$$

$$R^2 = 1 - \frac{\sum_{i=1}^{N}(X_{i,meas} - X_{i,pred})^2}{\sum_{i=1}^{N}(X_{i,meas} - \overline{X})^2} \quad (4)$$

Here $X_{i,meas}$, and $X_{i,pred}$ correspond to the actual and predicted values, respectively, while N indicates the total number of data points considered.

2.3. Linear multivariate regression models

In mining research, the linear multivariate regression (LMR) model is widely utilized to forecast hazardous outcomes arising from blasting activities [36-37]. This method establishes a relationship between a dependent variable and multiple independent variables by minimizing the discrepancies between observed and predicted values. Mathematically, the linear regression model can be expressed as:

$$Y = \{a_0 + a_1x_1 + ... + a_ix_i\} \quad (5)$$

where Y denotes the predicted output, a_0 is the intercept term, a_i (for i=1, 2, ..., n) are the coefficients corresponding to each predictor variable, and xi represent the input variables. Figure 3 illustrates the workflow of the LMR modeling approach.

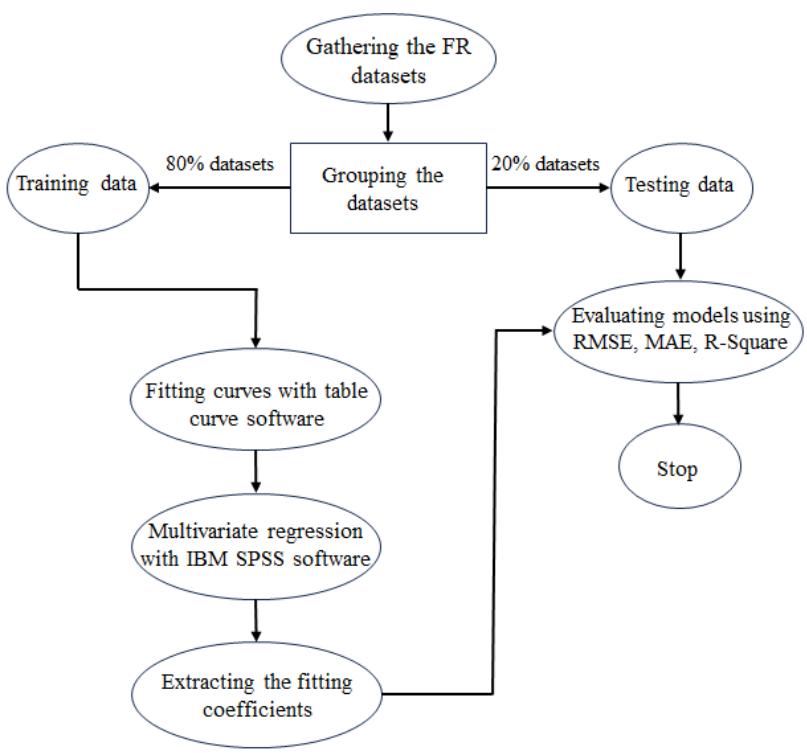

Figure 3. Flowchart of LMR mathematical model

2.4. Artificial neural network

Artificial Neural Networks (ANNs), first conceptualized by McCulloch and Pitts in 1943, are computational models inspired by the neural structures of the human brain [38]. A typical ANN architecture consists of three fundamental layers: the input layer, one or more hidden layers, and the output layer. Each layer contains neurons that process and relay information to subsequent layers. The determination of neuron counts per layer is usually performed through either heuristic approaches or systematic trial-and-error methods. Interconnections between neurons are weighted, modulating the strength of signals passed through the network by either amplifying or attenuating them. While a single hidden layer is often sufficient for solving relatively simple problems [39-40], complex datasets benefit from deeper networks containing multiple hidden layers capable of modeling sophisticated patterns [41]. Various neuron interconnection schemes exist, but among training algorithms, backpropagation (BP) remains the most prevalent and accessible technique [42-44]. ANN development involves two primary phases: architecture design and optimization of connection weights. The BP algorithm iteratively updates weights to reduce the discrepancy between predicted outputs and actual target values, continuing until the error converges below a predefined threshold, thereby enhancing prediction reliability. In this research, key input variables, including the number of blast holes (N), spacing (S), burden (B), specific drilling (SD), total charge (TC), specific charge (SC), and charge per hole (CPH), were used to predict the output variable, flyrock distance (FR). The employed ANN structure is illustrated in Figure 4.

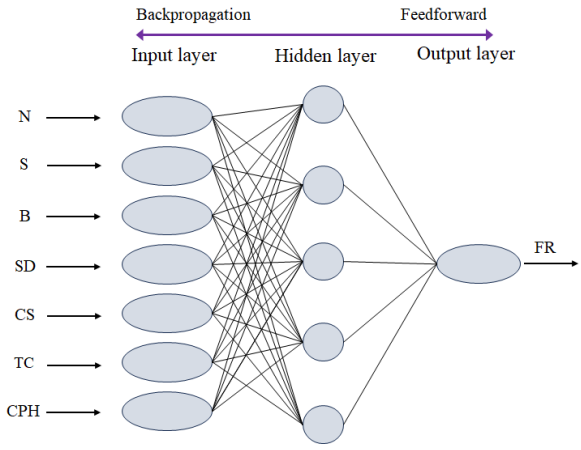

Figure 4. The basic framework of the ANN

2.5. Imperialist competitive algorithm

Introduced by Atashpaz-Gargari and Lucas in 2007, the Imperialist Competitive Algorithm (ICA) draws inspiration from socio-political dynamics [45]. Recognized for its rapid convergence and robust exploration capabilities in optimization problems, ICA has been widely adopted [24]. The ICA process, illustrated in Figure 5, initiates by generating a random population of countries, which are grouped into empires [46]. According to the population's cost function values, a subset of the strongest countries are designated as imperialists, while the rest become colonies. These imperialist nations then allocate colonies based on their relative power. Subsequently, a competition phase ensues, where dominant empires seize colonies from weaker ones. As colonies gain strength, the positions of empires and their colonies evolve dynamically, resulting in shifting balances of power. This iterative mechanism proceeds until a single empire prevails, signifying the elimination of all competing empires [24]. For further insights and technical details on ICA, refer to Koopialipoor et al. [19] and the original work by Atashpaz-Gargari and Lucas [45]. Figure 5 depicts the schematic flow of the ICA algorithm.

2.6. Ant colony optimization algorithm

The Ant Colony Optimization (ACO) algorithm, initially proposed by Dorigo in 1992, is inspired by the natural foraging behavior of real ant colonies searching for food sources [47]. Within the ACO framework, a group of artificial ants collaboratively explores potential solutions by indirectly communicating through the deposition of simulated pheromones. This approach employs a parallel search strategy, where multiple computational agents work simultaneously based on localized information of the problem space. Over time, the search is guided by the quality of discovered solutions, with a dynamic memory system playing a crucial role in the optimization procedure [48]. In this context, pheromones are linked to components of solutions and influence the decision-making of artificial ants as they construct new candidate solutions. The amount of pheromone deposited is adjusted during the run, reinforcing high-quality solutions and increasing the likelihood that subsequent ants will follow those paths. Simultaneously, pheromone evaporation reduces the influence of less optimal routes, preventing premature convergence on suboptimal solutions.

3. Results

3.1. Flyrock distance Prediction Using the LMR Model

The development of the Linear Multivariate Regression (LMR) model involved examining various combinations of input variables across multiple stages. This process was guided by insights obtained from the box plot analysis and the correlation matrix. Table 3 illustrates the Pearson correlation coefficients, which quantify the relationships between the predictor variables and the target output. According to the values reported in Table 2, a correlation coefficient of 0 signifies no linear association, while coefficients of -1 and 1 represent perfect negative and positive linear correlations, respectively.

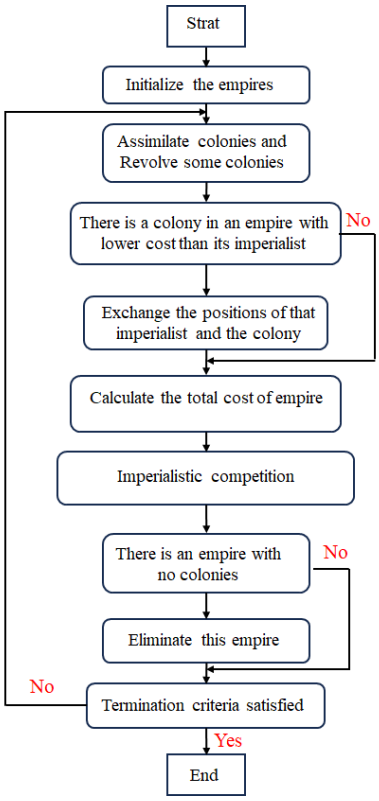

Figure 5. Flowchart of ICA algorithm

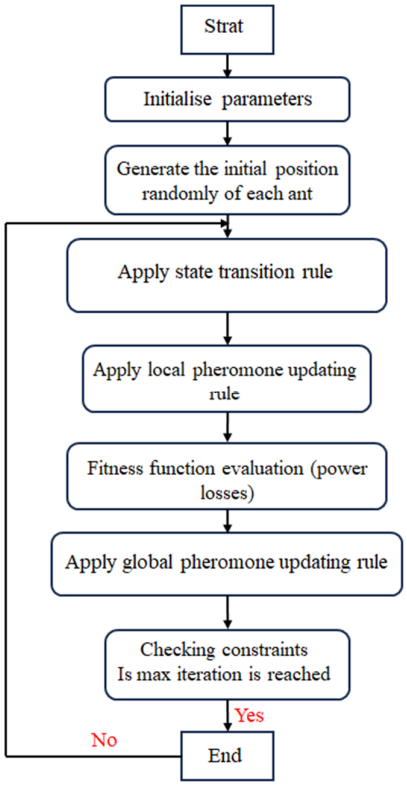

Figure 6. Flowchart of ACO algorithm

Table 3. The correlation matrix between inputs and output parameters.

	N	S	B	SD	TC	SC	CPH
N	1	0.134	0.134	-0.082	0.760	-0.041	0.126
S	0.134	1	0.952	-0.777	0.156	-0.723	-0.015
B	0.134	0.952	1	-0.777	0.156	-0.723	-0.015
SD	-0.082	-0.777	-0.777	1	0.090	0.947	0.046
TC	0.760	0.156	0.156	-0.090	1	0.064	0.049
SC	0.041	-0.723	-0.723	0.947	0.064	1	0.350
CPH	0.126	-0.015	-0.015	0.046	0.496	0.350	1

To identify the best multivariate regression model, a stepwise selection procedure was applied. This method aimed to find the optimal relationship among various candidate models. The evaluation relied on three key statistical metrics: (1) coefficient of determination (R^2), (2) Mean Absolute Error (MAE), and (3) Root Mean Square Error (RMSE). The goal was to maximize R^2 while minimizing both MAE and RMSE, thereby enhancing the model's predictive accuracy and robustness. The final LMR model, expressed in Equation (6), achieved an R^2 of 0.82, an MAE of 5.67 m, and an RMSE of 6.86 m for forecasting flyrock distance.

$$FR = 164.48 - (0.53 \times N) + (85.93 \times S) - (78.54 \times B) - (6788.52 \times SD) - (0.0007 \times TC) + (0.79 \times SC) - (15.78 \times CPH) \quad (6)$$

The variables considered in the model include Number of holes (N, dimensionless), Spacing (S, meters), Burden (B, meters), Specific Drilling (SD, m/m³), Total Charge (TC, kg), Specific Charge (SC, kg/m³), and Charge per Hole (CPH, kg). According to Equation (6), flyrock distance (FR) exhibits a positive correlation with spacing (S) and specific charge (SC). Conversely, number of holes (N), burden (B), specific drilling (SD), total charge (TC), and charge per hole (CPH) show a negative correlation with FR. Figure 7 demonstrates the comparison between the flyrock distances predicted by the LMR model and the actual measured values during both training and testing stages. The coefficient of determination (R^2) was 0.82 for the training data and 0.79 for the testing data. Additionally, the Root Mean Square Error (RMSE) was 8.09 m in the training phase and 6.86 m in the testing phase.

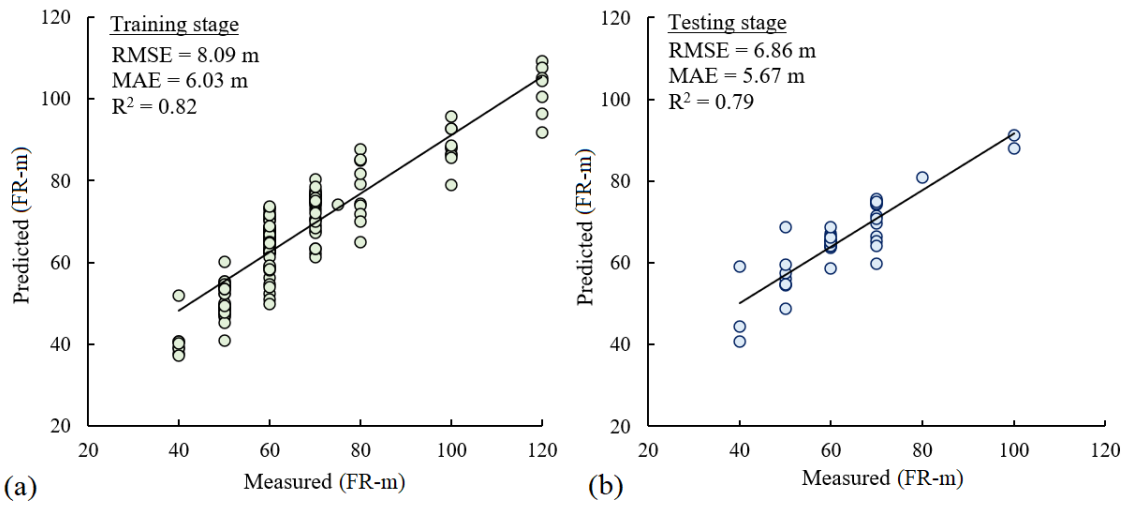

Figure 7. Correlation between measured and predicted FR in MLR model
a: Training phase b: Testing phase

3.2. Flyrock distance Prediction Using the ANN-MLP Model

To construct the optimized neural network, multiple random search-based optimization techniques were employed to determine the best combination of hyperparameters, including the number of hidden layers, neurons per layer, and activation functions. Numerous network architectures were rigorously evaluated, leading to the selection of a model featuring two hidden layers with five neurons each, utilizing sigmoid activation functions. The ANN-MLP was trained using the backpropagation algorithm with the Levenberg-Marquardt optimizer, a fixed learning rate of 0.01, and Mean Squared Error (MSE) as the loss function to guide weight updates. The network's predictive performance was assessed by comparing its outputs with experimental measurements, employing error metrics outlined in equations 2 through 4. These error values served as the key factors in choosing the most suitable architecture. Table 3 summarizes the configuration and hyperparameter details of the top-performing network. This strategy ensured the neural network was fine-tuned for optimal balance between accuracy and computational efficiency, making it the preferred choice for flyrock distance prediction.

Table 3. Parameters of optimum ANN-MLP model.

Optimal model	Number of hidden layers	Number of neurons per layer	Iterations	Data classification	RMSE (m)	MAE (m)	R^2
ANN-MLP	2	5	1000	20	9.31	7.10	0.81

Figure 8 presents a comparison between the predicted flyrock distances from the optimized ANN-MLP model and the observed measurements during both training and validation stages. The selected neural network demonstrated robust predictive capabilities, achieving an R^2 value of 0.86, a Mean Absolute Error (MAE) of 4.84 meters, and a Root Mean Square Error (RMSE) of 6.61 meters in the training phase. In the testing phase, the model sustained satisfactory accuracy, with an R^2 of 0.81, an MAE of 7.10 meters, and an RMSE of 9.31 meters.

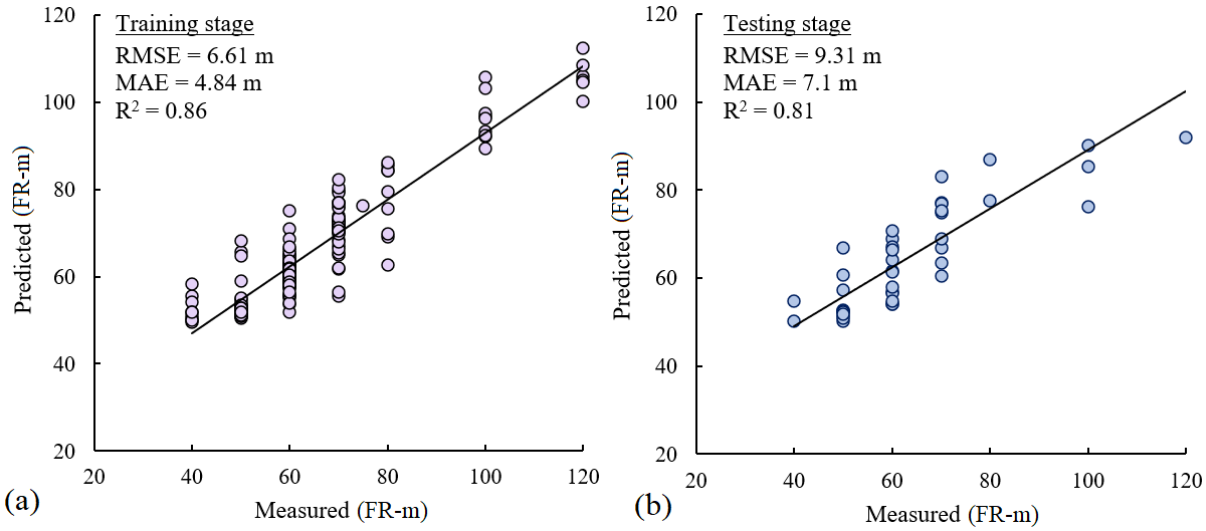

Figure 8. Correlation between measured and predicted FR in ANN-MLP model a: Training phase b: Testing phase

Figure 9 illustrates a detailed comparison between the flyrock distances predicted by the optimized ANN-MLP neural network and the actual measured distances during the testing phase. The results demonstrate that the ANN-MLP model provides precise predictions, closely aligning with the observed data. This confirms the model's ability to effectively learn and represent the complex relationships between input variables and flyrock distance, highlighting its reliability and strong forecasting performance.

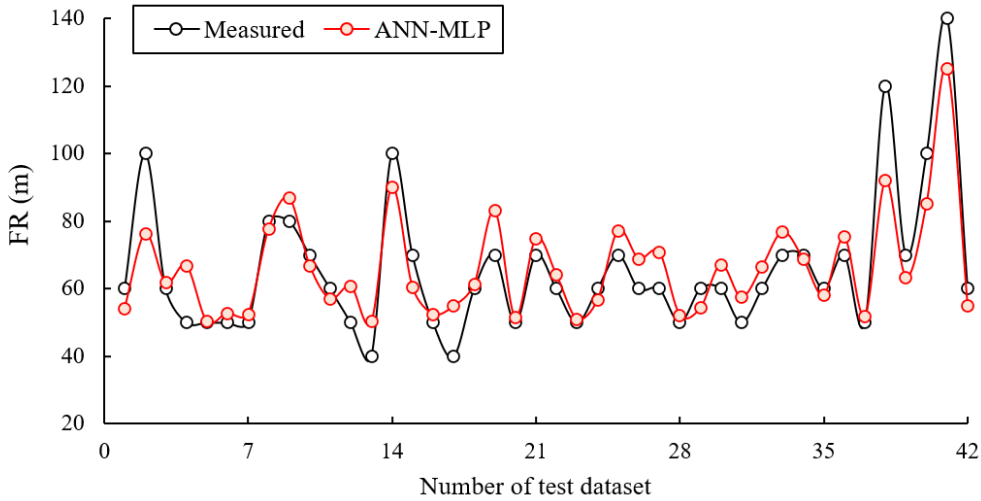

Figure 9. Evaluation of predicted versus observed flyrock distances during the testing phase using the ANN-MLP model

A crucial part of evaluating prediction models involves examining how sensitive the flyrock distance considered as the output is to changes in input variables. To measure the influence each

input factor exerts on the flyrock distance, the Relevancy Factor (RF) is utilized [29]. When there is a notable difference between the predicted and actual values, it generally suggests that the excluded parameter plays a significant role in affecting the model's results [49]. The RF is calculated using the following formula:

$$r(p_l, MMP) = \frac{\sum_{i=1}^{N}(p_{l,i} - \overline{p}_l)(MMP_i - \overline{MMP})}{\sqrt{\sum_{i=1}^{N}(p_{l,i} - \overline{p}_l)^2 \sum_{i=1}^{N}(MMP_i - \overline{MMP})^2}} \quad (7)$$

In this framework, $p_{l,i}$ and p_l denote the individual and mean values of the ith input variable, respectively, whereas MMP_i and MMP represent the predicted output's individual and average values. The RF value represents the degree to which variations in a given input variable explain variations in the model-predicted output. Positive RF values indicate that increases in the input tend to increase the output, whereas negative values imply an inverse relationship. Figure 10 shows the contribution of each input parameter to flyrock distance. Among the variables, total charge (TC), number of holes (N), and charge per hole (CPH) exhibit the highest influence at 17.36%, 16.26%, and 16.11%, respectively. These findings are in agreement with earlier research conducted by Armaghani et al. [2], Mohamad et al. [50], and Yari et al. [51]. Conversely, spacing (S) shows the lowest sensitivity at 11.45%, which aligns with the observations of Yari et al. [17]. This highlights the importance of carefully managing charge per hole, total charge, and hole count to enhance blasting effectiveness at the mine under investigation.

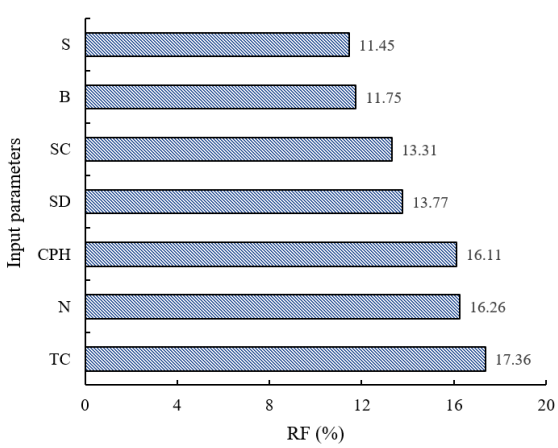

Figure 10. Sensitivity analysis illustrating the influence of input variables on flyrock distance prediction

3.3. Optimization of ANN Model Using ICA and ACO Algorithms

To enhance the performance of the neural network, the Imperialist Competitive Algorithm (ICA) and Ant Colony Optimization (ACO) were employed. These metaheuristic algorithms optimize the network by minimizing prediction error. They achieve this through adjustment of weights and biases, guided by an objective function. However, it is important to note that neither ICA nor ACO inherently optimize the neural network's architecture. Therefore, the best-performing ANN model identified in the previous section was utilized as the fixed network structure to serve as the objective function for both optimization algorithms. A critical aspect of implementing ICA and ACO involves tuning their control parameters, as these significantly affect the convergence speed and solution quality. Unlike conventional models, there are no strict formulas for setting these parameters; instead, expert insight combined with trial-and-error experimentation using the dataset is required to find optimal values. For ICA, key parameters include: Number of countries ($N_{country}$), Number of imperialists (N_{imp}), Maximum number of iterations (Max_{it}), Revolution rate (R_R), Revolution probability (R_p), Colonial mean cost coefficient (ζ), Assimilation coefficient (β). For ACO, the essential parameters are: Number of ants (N_{ant}), Initial pheromone value (τ_0), Pheromone exponential weight (α), Maximum number of iterations (Max_{it}), Heuristic exponential weight (β), Evaporation rate (ρ). Through extensive iterative testing, the optimal values for these parameters were identified and are summarized in Table 4. It should be noted that the control parameters of ICA and ACO are dimensionless. Their values were selected based on a combination of literature recommendations and trial-and-error tuning over the Sungun dataset. For instance, the assimilation coefficient ($\beta = 1.5$) in ICA determines the movement speed of colonies toward the imperialist; large β values hasten convergence but may overshoot optima, while small values slow convergence. Similarly, other parameters such as the pheromone exponential weight (α) and evaporation rate (ρ) in ACO adjust the balance between exploration and exploitation.

Table 4. Parameter values of ICA and ACO algorithms

Meta-heuristic algorithm	Hyperparameter	Description	Values
ICA	$N_{country}$	Number of countries	20
	N_{imp}	Number of imperialists	10
	It_{max}	Maximum number of iterations	1000
	R_R	Revolution Rate	0.1
	R_P	Revolution Probability	0.05
	ζ	Colonies Mean Cost Coefficient	0.2
	β	Assimilation Coefficient	1.5
ACO	N_{ant}	Number of ants	20
	It_{max}	Maximum number of iterations	1000
	Q	Contant	0.5
	τ_0	Initial pheromone	1
	α	Pheromone exponential weight	0.6
	β	Heuristic exponential weight	0.5
	ρ	Evaporation rate	0.1

Figure 11 compares the predicted and observed flyrock distances during the testing phase for the hybrid neural network models ICA-ANN and ACO-ANN. Both models perform very well when flyrock distances (FR) are low, showing strong prediction accuracy in this range. However, predicting peak FR distances remains challenging, with higher errors observed at these extreme values. This difficulty is partly due to the majority of the dataset falling within a limited range of 50 to 70 meters, which restricts the model's ability to accurately capture higher FR distances. As a result, the hybrid models exhibit decreased precision when estimating these larger flyrock distances. Despite these challenges, both hybrid ANN models show improved overall performance compared to previous models, with higher R^2 values and lower RMSE and MAE errors. Among them, the ICA-ANN model demonstrates superior predictive capability. During the training phase, it achieved an RMSE of 5.36 m, an MAE of 4.37 m, and an R^2 of 0.92. In the testing phase, the model maintained strong results with RMSE, MAE, and R^2 values of 5.66 m, 4.60 m, and 0.89, respectively. The ACO-ANN model followed closely, with training phase metrics of RMSE = 6.42 m, MAE = 5.29 m, and R^2 = 0.88, and testing phase values of RMSE = 6.76 m, MAE = 5.45 m, and R^2 = 0.84. Overall, these findings highlight the advantage of combining metaheuristic algorithms with ANNs, particularly emphasizing the effectiveness of the ICA-ANN approach in improving flyrock distance predictions. To demonstrate the effectiveness of the proposed hybrid ANN models (ICA-ANN and ACO-ANN), their performance was compared with previous studies at the Sungun Copper Mine [17, 33], which used DNNs optimized with JAYA, Multi-Verse, and Gravitational Search Algorithms, as well as tree-based models like AdaBoost, Random Forest, and XGBoost. Reported R^2 values ranged from 0.82 to 0.99. The ICA-ANN model achieved R^2 = 0.89, which is comparable or superior. Differences in performance metrics can be attributed to variations in input parameters, dataset size, and optimization methods. These results confirm that the hybrid ANN in this study effectively captures nonlinear relationships between blasting parameters and flyrock distances, achieving competitive R^2 and low RMSE, and demonstrating its reliability and practical applicability.

Figure 12 presents a radar chart comparing the evaluation metrics R^2, RMSE, and MAE for predicting flyrock distances during both the training and testing phases. This visual representation provides an overview of the overall performance of each model. In the radar chart, each axis corresponds to one performance metric, and the distance from the center reflects the magnitude of that metric. The ICA-ANN model consistently achieves the best results, showing the highest R^2 and the lowest RMSE and MAE values across both phases. Conversely, the MLR model exhibits the weakest predictive accuracy among the models assessed. The ACO-ANN model ranks second, demonstrating notable improvement over the baseline ANN. These findings confirm that incorporating optimization algorithms like ICA and ACO significantly enhances the predictive capability of ANN models for flyrock distance.

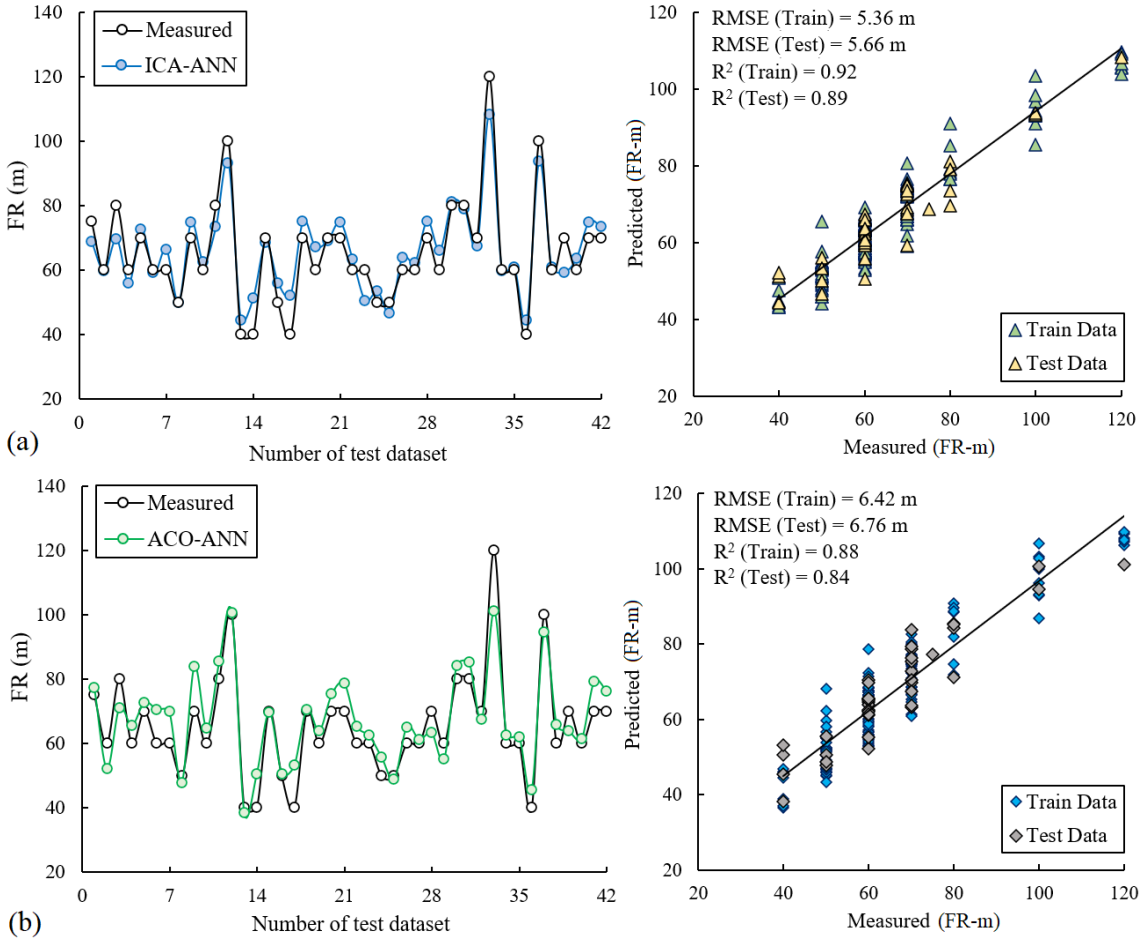

Figure 11. Correlation between measured and predicted flyrock distances (FR) and comparison of predicted versus measured FR values during the testing phase for; a: ICA-ANN model, b: ACO-ANN model

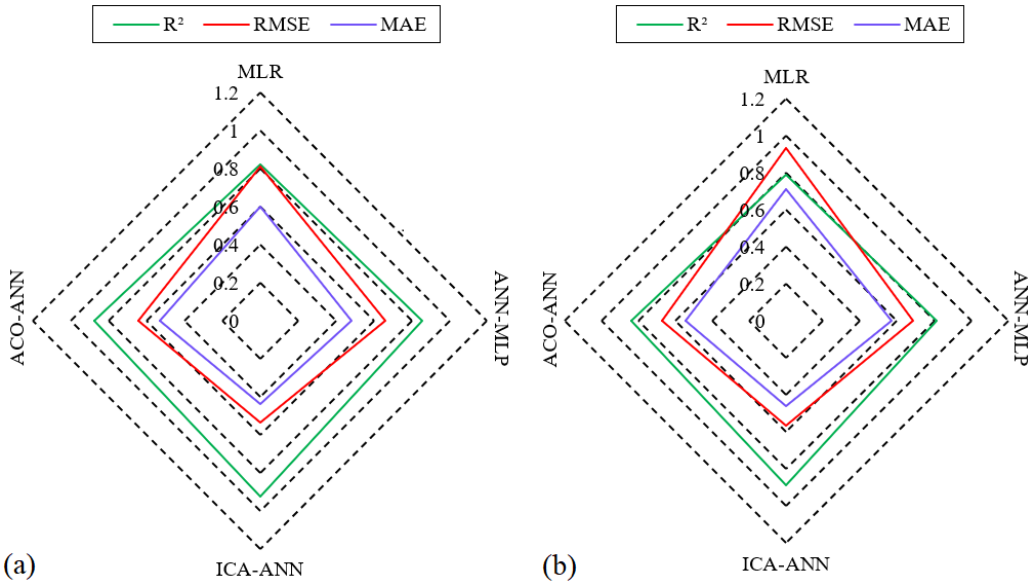

Figure 12. Radar diagram of the performance of models for prediction of FR (flyrock distance). Axes represent R² (dimensionless), RMSE (m), and MAE (m). a: Training phase; b: Testing phase.

Figure 13 shows a Taylor diagram comparing the measured and predicted flyrock distances for both training and testing phases. In the Taylor diagram, the radial distance represents the standard deviation, the angular position indicates the correlation coefficient, and the curved arcs depict the RMSE. This diagram allows simultaneous assessment of model performance using three key statistics: RMSE, standard deviation, and correlation coefficient, providing a comprehensive view of how well the predicted data align with observations. The x- and y-axes represent the standard deviation, while the curved arcs indicate RMSE values. Points closer to the reference location signify higher predictive accuracy and better agreement with actual measurements. According to the diagram, the ICA-ANN model shows superior performance over the ANN-MLP model in both phases. The overall ranking of models from best to worst is: ICA-ANN, ACO-ANN, ANN-MLP, and LMR.

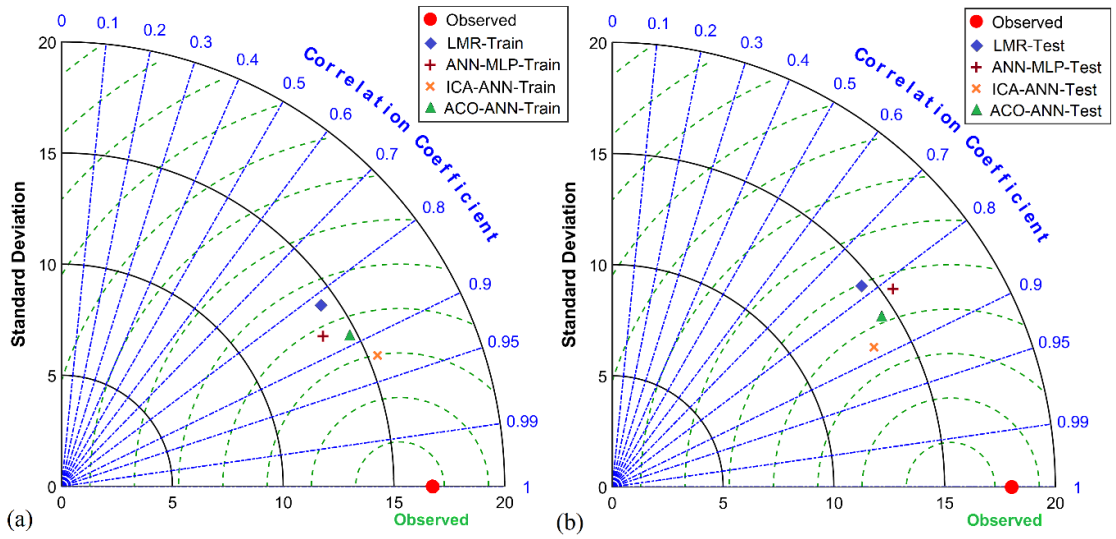

Figure 13. Taylor diagram illustrating the accuracy of the models during a: Training and b: Testing phases. The radial distance represents the standard deviation (m), the angular position corresponds to R^2 (dimensionless), and the curved arcs show RMSE (m).

3.4. Tail-Focused Performance Analysis

To further evaluate the robustness of the developed models, their predictive ability was assessed specifically in the upper tail of the flyrock distance (FR) distribution, where extreme and hazardous events occur. Tail performance was evaluated exclusively on the held-out test set to ensure that the reported metrics reflect the models' generalization ability rather than their fit to the training data. We computed RMSE and MAE not only for the entire testing dataset but also for the top decile (10%) of FR values. For the testing set (n = 42), this corresponds to the five largest FR values for each model. The results are summarized in Table 5. While all three models achieved acceptable accuracy on the full test set, their predictive performance noticeably deteriorated in the upper tail. The baseline ANN exhibited the weakest tail performance (RMSE_top10%=19.42 m, MAE_top10%=18.25 m), systematically underestimating long-range flyrock distance. In contrast, the ICA-ANN model demonstrated superior tail robustness (RMSE_top10%=8.65 m, MAE_top10%=8.34 m), followed by ACO-ANN (RMSE_top10%=9.94 m, MAE_top10%=7.83 m). Although the hybrid approaches significantly reduced error relative to the baseline ANN, even the best-performing model exhibited residual bias in extreme cases. Despite these improvements, the upper-tail errors remain markedly higher than the models' overall performance, reflecting the influence of data imbalance (the majority of FR values concentrated between 50–70 m) and the limited representation of extreme events in the training set. This pattern is consistent with observed residual distributions (Fig. 11), where deviations increase substantially at higher FR levels. Such limitations are critical, as high-range flyrock distance events generally involve greater velocities and present more severe safety and damage risks.

Table 5. Performance metrics for the full testing dataset and the upper tail (top 10% of FR values).

Model	RMSE (Full test) (m)	MAE (Full test) (m)	RMSE (Top 10%) (m)	MAE (Top 10%) (m)	Mean Bias in Top 10% (Pred−Obs) (m)	MAPE in Top 10% (%)
ANN-MLP	9.32	7.10	19.42	18.25	−18.25 (systematic underestimation)	16.48
ICA-ANN	5.66	4.61	8.65	8.34	−8.34	8.80
ACO-ANN	6.69	5.38	9.94	7.83	−5.43	7.92

4. Discussion

4.1. Model Evaluation and Performance

This study evaluated the effectiveness of advanced artificial intelligence (AI) and metaheuristic optimization algorithms in predicting flyrock distances at the Sungun Copper Mine in Iran. Multiple modeling frameworks were constructed, including linear multivariate regression (LMR), a conventional ANN-MLP, and two hybrid metaheuristic-optimized neural networks (ICA-ANN and ACO-ANN). The aim was to address the challenges of modeling highly nonlinear and uncertain flyrock phenomena.

The results showed that the hybrid ICA-ANN model achieved the highest predictive accuracy among all frameworks. Metaheuristic optimization improves ANN performance by effectively exploring the network's weight and bias space, enabling the model to capture complex nonlinear relationships between blasting parameters and flyrock distances. In contrast, linear multivariate regression is limited by linearity assumptions, and conventional ANN-MLP is prone to local minima, reducing predictive reliability.

4.2. Sensitivity Analysis and Influential Parameters

Sensitivity analysis revealed that the total charge (TC), the number of blast holes (N), and the charge per hole (CPH) are the most influential variables, collectively contributing more than half of the model's output variance. These results align with blasting physics: increasing explosive energy or the number of holes directly affects rock fragmentation and flyrock travel distance. Conversely, spacing (S) had the lowest impact, highlighting the importance of optimizing charge distribution and blast design.

4.3. Accuracy at Extreme Flyrock Distance Events

The observed decline in accuracy at the upper tail can be attributed to two main factors: (i) data imbalance, since the vast majority of blasting events fall within the range of 50–70 m and only a small number of long-range events exist in the dataset; and (ii) objective function bias, as conventional training criteria (e.g., mean squared error) place disproportionate emphasis on average performance while assigning little weight to extreme cases. As a result, the models exhibit a tendency to underestimate the magnitude of the most critical events, which undermines their practical safety value. These findings highlight the importance of integrating tail-focused training strategies in future work. Potential approaches include weighting schemes in the loss function to penalize underestimation of extreme values, targeted oversampling of long-range cases, and the adoption of quantile-based learning objectives to improve high-percentile accuracy. Moreover, incorporating prediction intervals and calibration diagnostics would enhance decision-support capabilities for practical blasting operations.

4.4. Limitations and Future Improvements

Additional limitations of the proposed model include manual ANN architecture selection, sensitivity to measurement noise in explosive parameters and spacing, and linearity assumptions in LMR. Future improvements could involve automated architecture optimization (AutoML), expanded datasets to capture extreme events, and the integration of explainable AI techniques to refine predictive performance. Overall, the findings highlight the potential of hybrid AI-metaheuristic models, particularly ICA-ANN, in providing robust, data-driven support for blast design and safety management. These models offer a reliable framework for enhancing operational safety and optimizing blasting parameters.

5. Conclusions

Flyrock distance (FR) is one of the most hazardous consequences of blasting in open-pit mining. This research focused on forecasting blast-induced flyrock distance at the Sungun Copper Mine using two metaheuristic optimization algorithms, the Imperialist Competitive Algorithm (ICA) and the Ant Colony Optimization (ACO), integrated with an optimized Artificial Neural Network-Multilayer Perceptron (ANN-MLP). A linear multivariate regression (LMR) model was

also developed as a baseline. The predictive models incorporated seven key input variables: the number of holes (N), spacing (S), burden (B), specific drilling (SD), total charge (TC), specific charge (SC), and charge per hole (CPH). Among all frameworks, the ICA-ANN model exhibited the best performance, demonstrating both statistical and practical advantage. Sensitivity analysis confirmed that TC, N, and CPH are the most influential factors, while spacing (S) had minimal effect. These insights highlight the importance of optimizing explosive energy input and blast hole configuration for safer and more efficient blasting operations.

Limitations include predictive errors for extreme flyrock events due to data imbalance, linearity assumptions in LMR, manual ANN architecture selection, sensitivity to measurement noise, and limited dataset size and diversity.

Future work should focus on testing the models on larger and more diverse datasets, automated ANN architecture optimization (AutoML), integration of additional geological and operational data, and prediction of related blasting phenomena such as ground vibrations and air overpressure. Implementing tail-sensitive training strategies and uncertainty quantification can further improve prediction accuracy for extreme flyrock events. Moreover, incorporating key blasting parameters such as hole diameter, inter-hole delay, and inter-row delay when variability is present would further enhance the robustness and comprehensiveness of predictive models.

Overall, this study demonstrates that hybrid AI-metaheuristic models, particularly ICA-ANN, provide robust, data-driven support for predicting flyrock distances, offering a practical and reliable alternative to conventional field-based prediction methods, and contributing to safer and more efficient blasting operations.

References

[1]. Singh, T. N., & Singh, V. (2005). An intelligent approach to prediction and control ground vibration in mines. *Geotechnical & Geological Engineering, 23*, 249–262.

[2]. Armaghani, D. J., Hajihassani, M., Mohamad, E. T., Marto, A., & Noorani, S. A. (2014). Blasting-induced flyrock and ground vibration prediction through an expert artificial neural network based on particle swarm optimization. *Arabian Journal of Geosciences, 7*, 5383–5396.

[3]. Faraji Asl, P., Monjezi, M., Hamidi, J. K., & Armaghani, D. J. (2018). Optimization of flyrock and rock fragmentation in the Tajareh limestone mine using metaheuristics method of firefly algorithm. *Engineering with Computers, 34*, 241–251.

[4]. Ladegaard-Pedersen, A., & Holmberg, R. (1973). The dependence of charge geometry on flyrock caused by crater effects in bench blasting. *Swedish Detonic Research Foundation Report DS*, 1–38.

[5]. Lundborg, N., Persson, A., Ladegaard-Pedersen, A., & Holmberg, R. (1975). Keeping the lid on flyrock in open-pit blasting. *Engineering and Mining Journal, 176*, 95–100.

[6]. Olofsson, S. O. (1990). Applied explosives technology for construction and mining. Arla, France: Applex Publisher.

[7]. Richards, A., & Moore, A. (2004). Flyrock control—by chance or design. In *Proceedings of the Annual Conference on Explosives and Blasting Technique* (Vol. 1, pp. 335–348). ISEE.

[8]. Monjezi, M., Rezaei, M., & Varjani, A. Y. (2009). Prediction of rock fragmentation due to blasting in Gol-E-Gohar iron mine using fuzzy logic. *International Journal of Rock Mechanics and Mining Sciences, 46*(8), 1273–1280.

[9]. Amini, H., Gholami, R., Monjezi, M., Torabi, S. R., & Zadhesh, J. (2012). Evaluation of flyrock phenomenon due to blasting operation by support vector machine. *Neural Computing and Applications, 21*, 2077–2085.

[10]. Marto, A., Hajihassani, M., Jahed Armaghani, D., Mohamad, E. T., & Makhtar, A. M. (2014). A novel approach for blast-induced flyrock prediction based on imperialist competitive algorithm and artificial neural network. *The Scientific World Journal, 2014*, 643715.

[11]. Faradonbeh, R. S., Jahed Armaghani, D., & Monjezi, M. (2016). Development of a new model for predicting flyrock distance in quarry blasting: A genetic programming technique. *Bulletin of Engineering Geology and the Environment, 75*, 993–1006.

[12]. Jahed Armaghani, D., Mohamad, E. T., Hajihassani, M., Alavi Nezhad Khalil Abad, S. V., Marto, A., & Moghaddam, M. R. (2016). Evaluation and prediction of flyrock resulting from blasting operations using empirical and computational methods. *Engineering with Computers, 32*, 109–121.

[13]. Nguyen, H., Bui, X. N., Bui, H. B., & Cuong, D. T. (2019). Developing an XGBoost model to predict blast-induced peak particle velocity in an open-pit mine: a case study. *Acta Geophysica, 67*(2), 477–490.

[14]. Nguyen, H., Bui, X. N., Bui, H. B., & Mai, N. L. (2020). A comparative study of artificial neural networks in predicting blast-induced air-blast overpressure at Deo Nai open-pit coal mine, Vietnam. *Neural Computing and Applications, 32*(8), 3939–3955.

[15]. Nguyen, H., Bui, X. N., & Moayedi, H. (2019). A comparison of advanced computational models and

experimental techniques in predicting blast-induced ground vibration in open-pit coal mine. *Acta Geophysica, 67*(4), 1025–1037.

[16]. Guo, H., Zhou, J., Koopialipoor, M., Jahed Armaghani, D., & Tahir, M. M. (2021). Deep neural network and whale optimization algorithm to assess flyrock induced by blasting. *Engineering with Computers, 37*, 173–186.

[17]. Yari, M., Armaghani, D. J., Maraveas, C., Ejlali, A. N., Mohamad, E. T., & Asteris, P. G. (2023). Several tree-based solutions for predicting flyrock distance due to mine blasting. *Applied Sciences, 13*(3), 1345.

[18]. Jiang, H., Zhang, Q., Li, T., Liu, X., & Zhang, Y. (2018). Prediction of flyrock distance using an artificial neural network (ANN) model. *Journal of Mining and Environment, 9*(10), 2197–2205.

[19]. Koopialipoor, M., Fallah, A., Armaghani, D. J., Azizi, A., & Mohamad, E. T. (2019). Three hybrid intelligent models in estimating flyrock distance resulting from blasting. *Engineering with Computers, 35*, 243–256.

[20]. Nguyen, H., Bui, X. N., Nguyen-Thoi, T., Ragam, P., & Moayedi, H. (2019). Toward a state-of-the-art of fly-rock prediction technology in open-pit mines using EANNs model. *Applied Sciences, 9*(21), 4554.

[21]. Rad, H. N., Hasanipanah, M., Rezaei, M., & Eghlim, A. L. (2018). Developing a least squares support vector machine for estimating the blast-induced flyrock. *Engineering with Computers*, *34*(4), 709-717.

[22]. Rezaei, M., Monjezi, M., Matinpoor, F., Bolbanabad, S. M., & Habibi, H. (2023). Simulation of induced flyrock due to open-pit blasting using the PCA-CART hybrid modeling. *Simulation Modelling Practice and Theory*, *129*, 102844.

[23]. Nikafshan Rad, H., Bakhshayeshi, I., Wan Jusoh, W. A., Tahir, M. M., & Foong, L. K. (2020). Prediction of flyrock in mine blasting: A new computational intelligence approach. *Natural Resources Research, 29*, 609–623.

[24]. Rezaei, M., Monjezi, M., & Varjani, A. Y. (2011). Development of a fuzzy model to predict flyrock in surface mining. *Safety science*, *49*(2), 298-305.

[25]. Zangoei, A., Monjezi, M., Armaghani, D. J., Mehrdanesh, A., & Ahmadian, S. (2022). Prediction and optimization of flyrock and oversize boulder induced by mine blasting using artificial intelligence techniques. *Environmental Earth Sciences, 81*(13), 359.

[26]. Zhou, Y., Zhang, X., Sun, X., Wang, S., & Shi, C. (2024). Advanced machine learning approaches for predicting flyrock using hybrid SVR models. *Computational Materials and Engineering, 140*(2), 56549.

[27]. Zhang, R., Li, Y., Gui, Y., Armaghani, D. J., & Yari, M. (2024). A stacked multiple kernel support vector machine for blast induced flyrock prediction. *Geohazard Mechanics, 2*(1), 37–48.

[28]. Kalaivaani, P. T., Akila, T., Tahir, M. M., Ahmed, M., & Surendar, A. (2020). A novel intelligent approach to simulate the blast-induced flyrock based on RFNN combined with PSO. *Engineering with Computers, 36*, 435–442.

[29]. Murlidhar, B. R., Nguyen, H., Rostami, J., Bui, X., Armaghani, D. J., Ragam, P., & Mohamad, E. T. (2021). Prediction of flyrock distance induced by mine blasting using a novel Harris Hawks optimization-based multi-layer perceptron neural network. *Journal of Rock Mechanics and Geotechnical Engineering, 13*(6), 1413–1427.

[30]. Hasanipanah, M., Keshtegar, B., Thai, D. K., & Truong, N. T. (2022). An ANN-adaptive dynamical harmony search algorithm to approximate the flyrock resulting from blasting. *Engineering with Computers*. Advance online publication, 1–3.

[31]. Ghasemi, A., & Zahediasl, S. (2012). Normality tests for statistical analysis: A guide for non-statisticians. *International Journal of Endocrinology and Metabolism, 10*(2), 486.

[32]. Aggarwal, V., Gupta, V., Singh, P., Sharma, K., & Sharma, N. (2019). Detection of spatial outlier by using improved Z-score test. In *2019 3rd International Conference on Trends in Electronics and Informatics (ICOEI)* (pp. 788–790). IEEE.

[33]. Ghojoghi, E., Farsangi, M. A. E., Mansouri, H., & Rashedi, E. (2024). Prediction and minimization of blasting flyrock distance, using deep neural networks and gravitational search algorithm, JAYA, and multi-verse optimization algorithms. *Heliyon*, *10*(19). 542.

[34]. Esmaeilzadeh, A., Shaffiee Haghshenas, S., Mikaeil, R., Guido, G., Shirani Faradonbeh, R., Abbasi Azghan, R., Jafarpour, A., & Taghizadeh, S. (2022). Risk assessment in quarries using failure modes and effects analysis method (case study: West-Azerbaijan mines). *Journal of Mining and Environment, 13*(3), 715–725.

[35]. Majedi-Asl, M., Ghaderi, A., Kouhdaragh, M., & Alavian, T. O. (2024). A performance comparison of the meta model methods for discharge coefficient prediction of labyrinth weirs. *Flow Measurement and Instrumentation, 96*, 102563.

[36]. Shakeri, J., Shokri, B. J., & Dehghani, H. (2020). Prediction of blast-induced ground vibration using gene expression programming (GEP), artificial neural networks (ANNs), and linear multivariate regression (LMR). *Archives of Mining Sciences, 65*(2).

[37]. Monjezi, M., Dehghani, H., Shakeri, J., & Mehrdanesh, A. (2021). Optimization of prediction of flyrock using linear multivariate regression (LMR) and gene expression programming (GEP)—Topal Novin mine, Iran. *Arabian Journal of Geosciences, 14*, 1–2.

[38]. McCulloch, W. S., & Pitts, W. (1943). A logical calculus of the ideas immanent in nervous activity. *The Bulletin of Mathematical Biophysics, 5*, 115–133.

[39]. Zhang, X., Nguyen, H., Bui, X. N., Tran, Q. H., Nguyen, D. A., Bui, D. T., & Moayedi, H. (2020). Novel soft computing model for predicting blast-induced ground vibration in open-pit mines based on particle swarm optimization and XGBoost. *Natural Resources Research, 29*(2), 711–721.

[40]. Norouzi, R., Daneshfaraz, R., & Ghaderi, A. (2019). Investigation of discharge coefficient of trapezoidal labyrinth weirs using artificial neural networks and support vector machines. *Applied Water Science, 9*, 1–10.

[41]. Nguyen, H., Bui, X. N., Tran, Q. H., Van Hoa, P., Nguyen, D. A., Hoa, L. T. T., … & Moayedi, H. (2020). A comparative study of empirical and ensemble machine learning algorithms in predicting air over-pressure in open-pit coal mine. *Acta Geophysica, 68*, 325-336.

[42]. Yilmaz, I., & Yuksek, A. G. (2008). An example of artificial neural network (ANN) application for indirect estimation of rock parameters. *Rock Mechanics and Rock Engineering, 41*(5), 781.

[43]. Hasanipanah, M., Noorian-Bidgoli, M., Jahed Armaghani, D., & Khamesi, H. (2016). Feasibility of PSO-ANN model for predicting surface settlement caused by tunneling. *Engineering with Computers, 32*, 705–715.

[45]. Dasineh, M., Ghaderi, A., Bagherzadeh, M., Ahmadi, M., & Kuriqi, A. (2021). Prediction of hydraulic jumps on a triangular bed roughness using numerical modeling and soft computing methods. *Mathematics, 9*(23), 3135.

[45]. Atashpaz-Gargari, E., & Lucas, C. (2007). Imperialist competitive algorithm: An algorithm for optimization inspired by imperialistic competition. In *2007 IEEE Congress on Evolutionary Computation* (pp. 4661–4667).

[46]. Alzoubi, I., Delavar, M., Mirzaei, F., & Nadjar Arrabi, B. (2017). Integrating artificial neural network and imperialist competitive algorithm (ICA) to predict the energy consumption for land leveling. *International Journal of Energy Sector Management, 11*(4), 522–540.

[47]. Dorigo, M. (1992). Optimization, learning and natural algorithms (Ph.D. thesis). Politecnico di Milano.

[48]. Hajizadeh, Y., Christie, M., & Demyanov, V. (2011). Ant colony optimization for history matching and uncertainty quantification of reservoir models. *Journal of Petroleum Science and Engineering, 77*(1), 78–92.

[49]. Oakley, J. E., & O'Hagan, A. (2004). Probabilistic sensitivity analysis of complex models: A Bayesian approach. *Journal of the Royal Statistical Society: Series B (Statistical Methodology), 66*(3), 751–769.

[50]. Mohamad, E. T., Armaghani, D. J., Noorani, S. A., Saad, R., Alvi, S. V., & Abad, N. K. (2012). Prediction of flyrock in boulder blasting using artificial neural network. *Electronic Journal of Geotechnical Engineering, 17*, 2585–2595.

[51]. Yari, M., Bagherpour, R., Jamali, S., & Shamsi, R. (2016). Development of a novel flyrock distance prediction model using BPNN for providing blasting operation safety. *Neural Computing and Applications, 27*, 699-706.

انجمن مهندسی معدن ایران
نشریه مهندسی معدن و محیط زیست
نشانی نشریه: www.jme.shahroodut.ac.ir
دانشگاه صنعتی شاهرود

پیش‌بینی پیشرفته پرتاب سنگ در عملیات آتشباری از طریق شبکه‌های عصبی مصنوعی و بهینه‌سازی فراابتکاری ترکیبی

جلیل حنیفه نیا[۱]، اکبر اسمعیل زاده[۲*]، صولت عطالو[۱] و رضا میکائیل[۱]

۱. گروه مهندسی معدن، واحد اهر، دانشگاه آزاد اسلامی، اهر، ایران
۲. گروه مهندسی معدن، دانشکده صنایع و فناوری های معدنی، دانشگاه صنعتی ارومیه، ارومیه، ایران
۳. گروه مهندسی معدن، واحد اهر، دانشگاه آزاد اسلامی، اهر، ایران
۴. گروه مهندسی معدن، دانشکده صنایع و فناوری های معدنی، دانشگاه صنعتی ارومیه، ارومیه، ایران

اطلاعات مقاله

تاریخ ارسال: ۲۰۲۵/۰۸/۰۹
تاریخ داوری: ۲۰۲۵/۰۸/۳۱
تاریخ پذیرش: ۲۰۲۵/۱۲/۲۵

DOI: 10.22044/jme.2025.16642.3261

کلمات کلیدی

پرتاب سنگ
مشکلات زیست محیطی
الگوریتم رقابت استعماری
بهینه سازی کلونی مورچه
معدن مس سونگون

چکیده

آتشباری تکنیکی حیاتی در استخراج معادن برای خرد کردن سنگ است، اما می‌تواند منجر به اثرات زیست‌محیطی مانند ارتعاشات، پرتاب سنگ و پس‌زدگی شود. پیش‌بینی و کنترل دقیق این اثرات برای بهبود ایمنی و به حداقل رساندن آسیب به تجهیزات و زیرساخت‌ها، ضروری است. هدف این تحقیق، پیش‌بینی فواصل پرتاب سنگ (FR) در معدن مس سونگون از طریق کاربرد مدل‌های هوش مصنوعی (AI) در ترکیب با رویکردهای آماری است. در ابتدا، یک مدل رگرسیون چند متغیره خطی (LMR) برای تعیین همبستگی بین پارامترهای آتشباری و دامنه پرتاب سنگ ساخته شد. پس از آن، یک شبکه عصبی مصنوعی مبتنی بر پرسپترون چند لایه (ANN-MLP) توسعه یافت و با استفاده از دو الگوریتم ترکیبی پیشرفته، یعنی الگوریتم رقابت استعماری (ICA) و بهینه‌سازی کلونی مورچگان (ACO) بهینه‌سازی شد. این الگوریتم‌ها برای کالیبره کردن وزن‌ها و بایاس‌های شبکه عصبی با استفاده از متغیرهایی مانند تعداد چال‌های انفجاری، فاصله چال‌ها، بار، کل بار، حفاری ویژه، بار در هر چال و بار ویژه به کار گرفته شدند. نتایج نشان داد که مدل ANN-MLP عملکرد بهتری نسبت به مدل LMR دارد، با معیارهای عملکرد خطای ریشه میانگین مربعات ($RMSE = 9.31$ متر)، خطای مطلق میانگین ($MAE = 7.10$ متر) و ضریب تعیین ($R^2 = 0.81$) در طول مرحله آزمایش. با این حال، بهینه‌سازی مدل ANN با ICA و ACO دقت پیش‌بینی را به طور قابل توجهی بهبود بخشید. در میان مدل‌های ترکیبی، مدل ICA-ANN بهترین عملکرد را با $RMSE = 5.66$ متر، $MAE = 4.60$ متر و $R^2 = 0.89$ نشان داد که بهبود قابل توجهی نسبت به مدل‌های LMR و ANN-MLP دارد. تجزیه و تحلیل حساسیت همچنین بار کل و تعداد چال‌ها را به عنوان مهم‌ترین پارامترهای مؤثر بر پراکندگی پرتاب سنگ برجسته کرد. به طور کلی، یافته‌ها بر پتانسیل چارچوب‌های هوش مصنوعی ترکیبی در پیشبرد مدل‌سازی پیش‌بینی برای عملیات آتشباری ایمن‌تر و کارآمدتر تأکید می‌کنند.

نویسنده مسئول مکاتبات: aesmail.1985@gmail.com (ا. اسمعیل زاده)